

---

CHEMICAL PHYSICS  
OF NANOMATERIALS

---

## Molecular Mechanism of the Spontaneous Segregation of Enantiomers in Liquid Nanoblobs

D. V. Zlenko<sup>a, b, \*</sup>, M. A. Tregubova<sup>b</sup>, and S. V. Stovbun<sup>b</sup>

<sup>a</sup>*Lomonosov Moscow State University, Moscow, 119991 Russia*

<sup>b</sup>*Semenov Institute of Chemical Physics, Russian Academy of Sciences, Moscow, 119991 Russia*

\**e-mail: dvzlenko@gmail.com*

Received May 25, 2016

**Abstract**—At present, the problem of spontaneous segregation has no satisfactory theoretical description. The main difficulty is a very low probability of the spontaneous formation of a chirally pure nucleus in a racemic mixture if the enantioselectivity energy is below  $(10–12)kT$ , which does not correspond to reality. In this paper, we propose a mechanism of the enhancement of enantioselectivity in the chiral phase nucleus, which circumvents the problem of the low probability of its formation.

**Keywords:** chirality, spontaneous segregation, molecular modeling, enantiomer excess

**DOI:** 10.1134/S1990793117020129

### INTRODUCTION

The onset of chiral purity, inherent to biological systems, in an initially racemic or weakly chirally polarized prebiotic world is one of the fundamental problems of natural sciences, dating back to Louis Pasteur [1], but still attracting many researchers [2–4], which, however, has not yet received a generally acceptable solution.

The formation of a chirally pure biological environment was most thoroughly studied by V.I. Gol'danskii et al. [5–8] (hereinafter, Gol'danskii model). Let us briefly summarize the main results of their theoretical treatment, highlighting the basic underlying assumptions. In the Gol'danskii model, prebiotic macromolecules are considered as a sequence of permanent chiral (*L* or *D*) monomer units (a few tens of units for prebiotic macromolecules and from  $\sim 10^2$  to  $\sim 10^6–10^7$  for biological molecules). The formation of macromolecules occurs in a racemic or weakly chirally polarized solution of monomers with opposite chiralities (antipodes) through consecutive, statistically independent events of attachment of units to a linear molecular chain. The free energies of attachment of an *L* or *D* isomer to the terminal unit of the assembled macromolecule are generally different, with the difference between the energies of attachment of a monomer of like and opposite sign is called the enantioselectivity energy  $W$ .

The main quantitative result of the Gol'danskii model is that the length of spontaneously formed homochiral polymer chains is determined by the enantioselectivity energy:  $W > kT \ln N$ , where  $N$  is the

length of the chain. Even at  $N \sim 10^2–10^3$ , the value of  $W$  should be at least  $(6–7)kT$ , whereas that for actually observed chains of length  $N \sim 10^6–10^7$ , the enantioselectivity energy should be  $(14–16)kT$ . Such a value of the enantioselectivity energy in biological systems is provided by the stereospecificity of operation of enzymes, which is fundamentally unattainable in their absence.

As a result Gol'danskii et al. discovered a paradoxical effect, which they called the chiral catastrophe. Indeed, to assemble a sufficiently long homochiral molecular chain in a solution of chiral monomers without using enantioselective enzymes, a chirally pure medium is needed. On the other hand, to achieve a desired degree of chiral purity, it is necessary to provide a very high enantioselectivity of the relevant physicochemical processes, which is associated with specific biological molecules. In the above discussion, the hypothetical physicochemical mechanism of the formation of a primary chirally pure medium or long homochiral primary linear macromolecules that would provide the required enantioselectivity in the original racemic or chiral weakly polarized environment seems confusing or even paradoxical.

Thus, the mechanism of the spontaneous segregation of enantiomers remains unclear. At the same time, it has a very large fundamental importance, since it underlies the process of emergence of homochiral macromolecules and likely the origin of life.

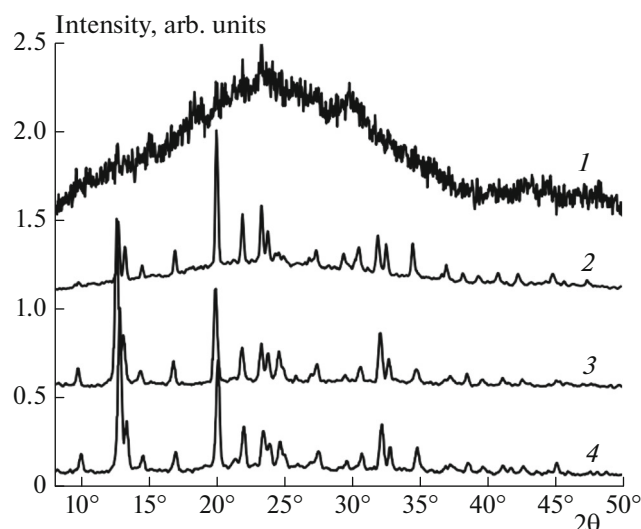


**Fig. 1.** Diffraction patterns of viscous residues formed after evaporation of the solvent from solutions of TFAAA-5 in heptane (4 mg/mL): (1) racemic solution, (2) 7 : 3 mixture of *L*- and *D*-enantiomers, (3) pure *D*-enantiomer, and (4) pure *L*-enantiomer.

## METHODS

We investigated xerogels of *N,N,N*-(trifluoroacetyl)aminoethanol [9], obtained by drying the solvent (heptane and cyclohexane). A MIKMED 6 optical microscope (Russia) was used to determine the concentration threshold  $C^*$  of formation of strings below which strings in the xerogel were not detected upon viewing more than 1000 independent fields, but above which strings were formed in large number.

The xerogel samples were analyzed on a modernized DRON-3 X-ray diffractometer (Russia) with a copper anticathode at a voltage of 30 kV, a current strength of 20 mA (Ni filter), and room temperature. The original sample was placed in a flat glass cell 10 mm in diameter and 1 mm in depth, which was positioned under a plane-parallel X-ray beam so as to ensure the reflection operation mode, and diffraction spectra were recorded.

Molecular dynamics (MD) calculations were performed using the GROMACS-5.0.5 software package [9] in combination with the OPLS-AA force field [10]. The integration step in all calculations was 1 fs. To perform calculations for long-range electrostatic interactions, the PME method [11] with a standard set of parameters (interpolation order, 4; lattice spacing, 1.2 Å) was used. The radii of truncation of short-electrostatic and dispersion interactions and of lists of neighboring atoms were 1.25 nm. All the calculations were performed with periodic boundary conditions at 300 K and an isotropic constant pressure of 1 atm. The process of constructing models of the molecules trifluoroacetylated amino alcohols (TFAAA) and solvent molecules was described in [12]. In the initial state,

TFAAA molecules in random orientations were placed 2 nm apart at sites of a cubic lattice [12]. The space between the TFAAA molecules was filled with solvent molecule pre-relaxed for 100 ns. The final model arrangement contained 216 TFAAA molecules in a 1728-nm<sup>3</sup> volume, which corresponds to a concentration of 0.2 M. For each arrangement, we performed molecular dynamics calculations for 100 ns; the second halves of the MD trajectories were used for analysis.

## RESULTS AND DISCUSSION

### *Experimental Observation of Spontaneous Segregation*

Previously, we have experimentally established that, in dilute homochiral TFAAA solutions, supramolecular strings with a constant diameter of  $\sim 1 \mu\text{m}$  and a length of up to 1 mm are formed [13, 14]. The formation of strings is a threshold phenomenon, which means that, below a certain critical concentration  $C^*$ , strings are not formed. Strings, woven from micrometer-diameter of 1- to 2-nm-diameter elementary strings, are homochiral; they contain no solvent and exhibit crystalline order [15–17]. Thus, elementary strings are similar to prebiotic molecules, as defined by the Gol'danskii model.

Diffractograms of xerogels of solutions of TFAAA *L*- and *D*-enantiomers in cyclohexane and heptane showed that the crystal lattices of both types of strings are identical (Fig. 1), although they have opposite chirality, as evidenced by the opposite signs of circular dichroism in homochiral TFAAA solutions of opposite chiralities (Fig. 2).

Racemic solutions of TFAAA-5 in heptane and cyclohexane behave fundamentally differently. It was found that, in a racemic solution of TFAAA-5 in heptane, strings are not formed: the evaporation of the solvent results in the formation of a viscous residue, which does not dry out completely for months and has a diffraction pattern characteristic of amorphous materials (Fig. 1). In this case, according to Gol'danskii's terminology [8], a physicochemical annihilation of antipodes takes place. At the same time, if the difference in the concentrations of the enantiomers (enantiomeric excess (EE)) exceeds the critical concentration  $C^*$  [13, 14], strings are formed. The diffractograms of the xerogel (Fig. 1) shows that the crystal lattices of strings formed in solutions with different EE are identical. This, in turn, means that all the strings are homochiral.

Thus, in the presence of a certain amount of enantiomers of opposite signs in a heptane solution, the latter annihilate to form a precipitate, while in an enantiomerically pure precipitate, homochiral strings of the same sign are formed, corresponding to the sign of EE. Indeed, if homochiral strings of both chirality signs were formed in the solution, in a truly racemic solution, strings would be also formed, which contradicts to observations.

At the same time, in a solution of racemic TFAAA-5 in cyclohexane, unlike in its solution in heptane, string formation takes place. Moreover, the critical concentration  $C^*$  for a racemic solution is twice higher, and diffractograms of xerogels prepared from homochiral and racemic solutions are identical; i.e., left and right string are formed independently of each other. Thus, in this system, a true spontaneous segregation of enantiomers takes place, which occurs even at a nearly zero EE.

Since the number of strings observed in a single capillary is small, tens or hundreds, the absence of strings in the racemic TFAAA-5 solution in heptane indicates only that strings are not formed. However, it does not mean that spontaneous segregation does not occur in an unstructured precipitate. To understand the nature of the observed phenomenon, it is worthwhile to carry out a molecular dynamics modeling of early stages of aggregation of TFAAA-5 molecules in heptane and cyclohexane, which precedes the formation of both a precipitate and strings.

#### Modeling of Spontaneous Segregation

As demonstrated in [12, 18], in highly dilute homochiral solutions, TFAAA molecules form liquid nanoblobs. As part of the present work, we performed MD simulations of the evolution of an initially homogeneous state in which TFAAA enantiomers of opposite signs are evenly distributed in space. Analysis of the composition of these nanoblobs makes it possible to draw conclusions about the energy of interaction of enantiomer molecules of like and unlike signs in heptane and cyclohexane.

As is the case with homochiral solutions, in racemic solutions, nanoblobs containing both enantiomers are formed. Analysis of the enantiomeric composition of these nanoblobs (for all the systems simulated) shows that, on the average, small nanoblobs (3–5 molecules) have no asymmetry in their composition. By contrast, in larger droplets (7–10 molecules), in both cyclohexane and heptane, a pronounced excess of one of the enantiomers is observed (Fig. 3). Note that, on the average, for all the systems studied, the formation of large droplets enriched in left or right TFAAA enantiomers is equally possible. Thus, the formation of a nanodroplet enriched in either enantiomer is a random event.

The probability of the random formation of asymmetric nanoblobs is large enough due to their small size. Indeed, the probability of the formation of a homochiral droplet consisting of  $n$  molecules in a racemic solution (assuming an equal probability of the attachment of both enantiomers) is

$$p = \left(\frac{1}{2}\right)^{n-1}.$$

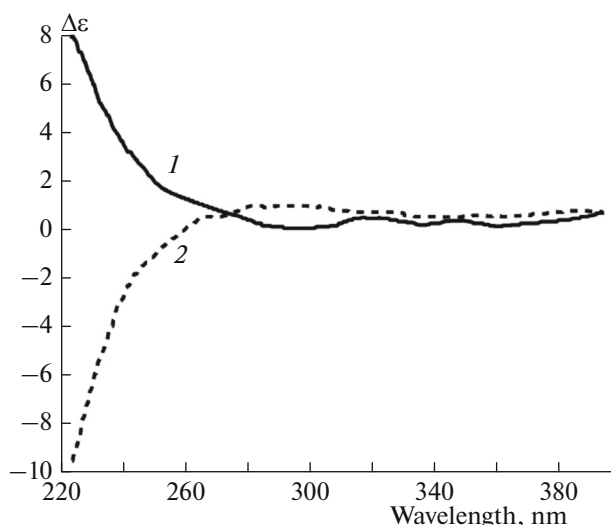


Fig. 2. Circular dichroism spectra  $\Delta\epsilon$  of homochiral (1) *L*- and (2) *D*-xerogels of TFAAA-5 (0.4 mg/mL) in heptane obtained by evaporation of the hexane solvent.

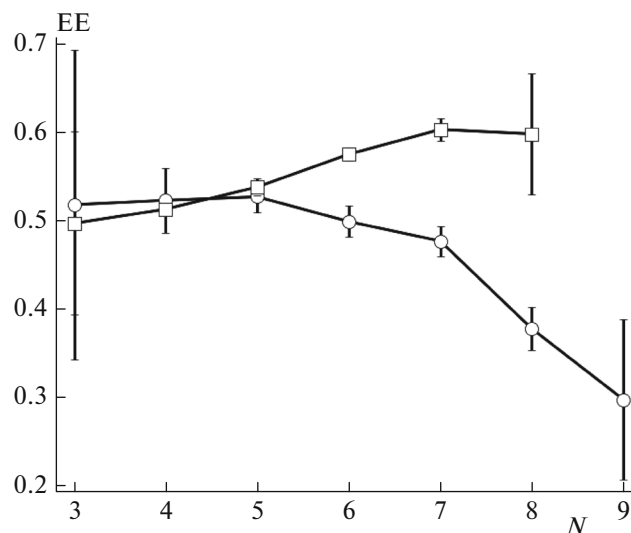
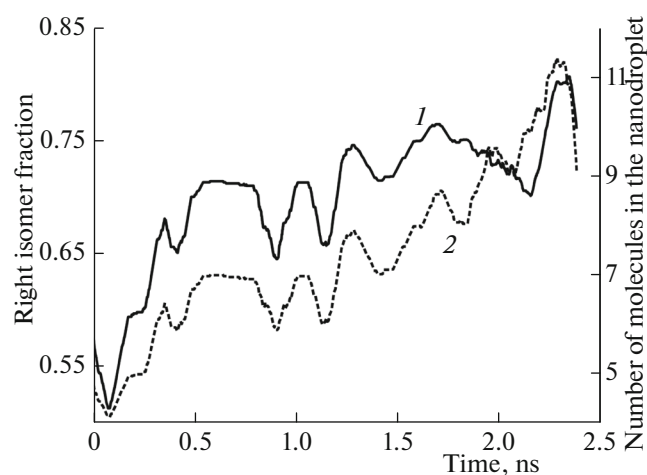


Fig. 3. Proportion of *D*-isomer in the composition of nanoblobs in a racemic solution of TFAAA-5 in (○) heptane and (□) cyclohexane. It is clearly seen that large droplets have a pronounced asymmetry in the number of left and right molecules.

Thus, the probability of the formation of a homochiral droplet consisting of 10 molecules is ~0.2%. By contrast, the probability of the formation of a symmetric droplet of the same size is about 25%, with the rest falling on droplets with partial asymmetry (6 : 4, 7 : 3, etc.). Thus, the mere fact that simulations predict the existence of asymmetric droplets looks quite expected.

If the enantioselectivity energy is zero, averaging over a sufficiently large ensemble must inevitably lead to a strictly symmetrical distribution of nanodroplet composition. If the enantioselectivity energy is high,



**Fig. 4.** Growth of the asymmetry of the nanodroplet composition. (1) The proportion of *D*-isomer in the composition of a large nanodroplet and (2) its size. It is clearly seen that, with increasing size of the nanodroplet, its composition is selectively enriched in one of the enantiomers.

the nanodroplet composition distribution should be bimodal. Both of these cases do not correspond to the picture we observe in numerical experiments. Large nanoblobs turn out to be enriched in either right or left enantiomers, which can be interpreted from a methodological point as the sample being unrepresentative. However, the observed effect makes it possible to draw a very interesting conclusion.

Because nanoblobs are characterized by a well-developed internal molecular dynamics [12], TFAAA molecules are free to leave them or join them again. Therefore, when counting the number of drops, we take into account all the realizations of the composition of each individual nanodroplet. In other words, we considered the evaporation or condensation of molecules not only as a change in the composition of the existing droplet, but as the emergence of a new droplet with a new composition, and take account of it in the statistics. Since large droplets have long lifetimes [12], the observed asymmetry of the composition of large droplets reflects the evolution of a small number of nanoblobs in the model solution, during which their asymmetries are enhanced, not attenuated. The number of long-lived droplets really should be small, because otherwise we would not have observed asymmetry due to averaging over a large number of large droplets.

If the enantioselectivity energy would be zero, then, with increasing size of a droplet, its asymmetry would have to disappear. Direct calculations show that, on the average, for large (more than 7 molecules) TFAAA-5 droplets in heptane and cyclohexane, the energy enantioselectivity is about 1 kJ/mol. According to Gol'danskii and Avetisov's evaluations, this value is absolutely insufficient for the formation of a chirally pure structure [5–7]. However, between the model

discussed by Gol'danskii, and the nanoblobs considered, there is a fundamental difference. The Gol'danskii model deals with a hard linear molecule, so if a “wrong-sign” enantiomer entered into its composition, the “error” could not be fixed. Accordingly, the enantioselectivity energy needed to be large enough so that the probability of attachment of even one “wrong” molecule would be negligibly small. At the same time, for a nanodroplet the composition of which continuously changes due to the dissociation and condensation of molecules, this constitutes no problem, since the molecules are constantly moving, interacting, swapping positions, and interacting arbitrarily. Consequently, the energy enantioselectivity must be considered not per molecule, but rather per nanodroplet as a whole. With this approach, for droplets consisting of 10 molecules, the enantioselectivity energy can be estimated as  $4kT$ . With increasing droplet size, it only increases, which results in a very significant reduction in the total energy of the system. This mechanism explains why our simulations predict an enhancement in the asymmetry of large nanoblobs and can generally explain the phenomenon of spontaneous segregation at low enantioselectivity energies.

Within the framework of the MD method, the proposed hypothesis can be tested directly. If the above mechanism is operative in simulations, then there must exist, even a few, large drops, the asymmetry of which increases with their size. That the number of strings observed in experiment is always small [13–15] suggests that the formation of a string is quite a rare event. Consequently, not all the nanoblobs produced in simulations must demonstrate an enhancement in enantioselectivity. Nevertheless, such droplets, in a small amount, must be present in the system. As can be clearly seen from Fig. 4, large droplets can actually exhibit the process of asymmetry enhancement. A nanodroplet composed of five molecules at the beginning of its existence, three of which were *D*-enantiomers and two, *L*-enantiomers, has grown to 11 molecules within 2.5 ns, 9.5 molecules of which are, on the average, *D*-enantiomers.

Thus, a key condition for spontaneous segregation at low ( $<kT$ ) enantioselectivity energy is the non-crystallinity of the elementary nucleus, which must be liquid. It is this requirement that is satisfied by nanoblobs we experimentally observed in [12, 18], nanoblobs in which a developed internal dynamics of the molecules, due to many collisions, makes it possible to obtain the effect of asymmetry of the enantiomeric composition, obviously preceding spontaneous segregation.

## CONCLUSIONS

Thus, the results of molecular dynamics simulations of the nanosized fraction of the dispersed phase observed in racemic solutions of TFAAA made it possible to reveal the spontaneous segregation of enantio-

mers. The effects observed indicate that, as the size of the dispersed phase particle increases, so does the enantioselectivity energy. This effect is associated with the liquid aggregate state of the droplet, for which the energy enantioselectivity should be regarded per nanodroplet as a whole rather than per molecule. This leads to the cumulative growth of the enantioselectivity energy with increasing size of the nucleus, which explains why large chirally pure nuclei are formed, a phenomenon that have not been satisfactorily explained previously.

#### ACKNOWLEDGMENTS

MD calculations were performed on the Lomonosov supercomputer at the Supercomputer Center of the Research Computer Center of Moscow State University.

#### REFERENCES

1. L. Pasteur, *Selected Works*, Ed. by A. A. Imshenetskii (Akad. Nauk SSSR, Moscow, 1960) [in Russian].
2. L. V. Yakovenko and V. A. Tverdislov, *Biophysics* **48**, 1053 (2003).
3. E. Broda, *Origins Life Evol. Biosphere* **14**, 391 (1984).
4. N. Fujii and T. Saito, *Chem. Rec.* **4**, 267 (2004).
5. V. A. Avetisov and V. I. Gol'danskii, *Phys. Usp.* **39**, 819 (1996).
6. V. A. Avetisov and V. I. Gol'danskii, *Khim. Fiz.* **16** (8), 59 (1997).
7. V. A. Avetisov, *Khim. Fiz.* **22** (2), 16 (2003).
8. V. I. Gol'danskii and V. V. Kuz'min, *Sov. Phys. Usp.* **32**, 1 (1989).
9. S. Pronk, S. Paul, R. Schutz, et al., *Bioinformatics* **29**, 845 (2013).
10. W. L. Jorgensen, D. S. Maxwell, and J. Tirado-Rives, *J. Am. Chem. Soc.* **118**, 11225 (1996).
11. U. Essmann, L. Perera, M. Berkowitz, et al., *Chem. Phys.* **103**, 8577 (1995).
12. D. V. Zlenko and S. V. Stovbun, *Russ. J. Phys. Chem. B* **9**, 667 (2015).
13. R. G. Kostyanovsky, D. F. Lenev, O. N. Krutius, and A. A. Stankevich, *Mendeleev Commun.* **15** (4), 140 (2005).
14. S. V. Stovbun, A. M. Zanin, A. A. Skoblin, A. I. Mikhailov, and A. A. Berlin, *Dokl. Phys. Chem.* **442**, 36 (2012).
15. S. V. Stovbun and A. A. Skoblin, *Mosc. Univ. Phys. Bull.* **67**, 317 (2012).
16. Ya. A. Litvin, A. N. Shchegolikhin, A. A. Skoblin, and S. V. Stovbun, *Russ. J. Phys. Chem. B* **10**, 725 (2016).
17. S. V. Stovbun, A. A. Skoblin, A. M. Zanin, D. P. Shashkin, V. A. Tverdislov, and A. A. Berlin, *Dokl. Phys. Chem.* **450**, 138 (2013).
18. S. V. Stovbun, A. A. Skoblin, A. M. Zanin, D. P. Shashkin, A. I. Mikhailov, M. V. Grishin, and B. R. Shub, *Russ. J. Phys. Chem. B* **7**, 1 (2013).

*Translated by V. Smirnov*